Superposition and Decomposition Analysis of Limbs' Vibration Based on 6-UPS Tibia Fracture Reduction Surgical Robot

Zhenyi Wang, Hongjian Yu*, Xiangyu Shen, Dongru Xie, Hao Wang and Zhijiang Du
State Key Laboratory of Robotics and Systems, Harbin Institute of Technology, Harbin, China

Keywords: 6-UPS Parallel Robot, Tibial Fracture Reduction Robot, Linear Vibration Units, Vibration Analysis, Dynamics Analysis.

Abstract: This article establishes the inverse kinematic model and forward kinematic model of the 6-UPS Stewart platform. Based on the existing 6-UPS tibial fracture reduction robot, the characteristics of the linear vibration unit and its installation on the robot limbs are analyzed. Under the condition that the moving platform outputs vibration along the force line direction, the superposition conditions of vibration in each limb are verified through forward kinematics, and the basic conditions for vibration synthesis are solved. Then, based on inverse kinematics, the desired vibration of the moving platform is decomposed to obtain the vibration equations that need to be output by the linear vibration units on each limb. Finally, combined with the Newton-Euler method, the robot dynamics are analyzed, and the model is imported into ADAMS for simulation verification, providing a theoretical basis for realizing the rehabilitation function of the 6-UPS tibial fracture reduction robot by adding linear vibration units.

1 INTRODUCTION

In recent years, the incidence of traumatic orthopedic diseases has increased. The fracture reduction surgery robot system can assist doctors in better realizing the accurate planning and real-time guidance of fracture reduction so that patients have better reduction results. The existing fracture reduction surgery robot mainly focuses on the reduction function (Ye, 2012). Ralf Westphal et al. from Germany developed a surgical reduction robot system for long bone fractures (Westphal R - Liodakis E). The robot adopts a typical industrial robot structure to operate on the fractured part of the patient. Terry K.K. Koo et al. proposed a computer-assisted fracture reduction method in 2006, which was powered by a unilateral external fixator to reduce long bone fractures (Koo, 2006). Hu Lei's team from Beihang University and the Chinese People's Liberation Army General Hospital jointly developed a fracture reduction robot system for the lower extremity tibia (Li C, 2016). However, the above studies do not consider postoperative rehabilitation. Cai Chenxu's research on mechanical vibration promoting bone cell growth shows that low-amplitude high-frequency vibration, as a non-invasive and safe treatment method, can effectively shorten fracture healing time, promote fracture healing, and have good effects on early-stage fracture healing (Cai C, 2023). But there has been no suitable solution for effectively combining fracture reduction with functional rehabilitation.

This article presents the inverse kinematic model and forward kinematic model for the 6-UPS Stewart platform. It analyzes the characteristics of a linear vibration unit and its installation on a 6-UPS tibial fracture reduction robot. The article verifies the superposition conditions of vibration in each limb through forward kinematics when the moving platform outputs vibration along the force line direction. It solves the basic conditions for vibration synthesis. Using inverse kinematics, the desired vibration of the moving platform is decomposed to determine the vibration equations that need to be output by the linear vibration units on each limb. The robot dynamics are then analyzed using the Newton-Euler method and the model is simulated and verified in ADAMS. The findings provide a theoretical basis for incorporating linear vibration units to achieve the rehabilitation function of the 6-UPS tibial fracture reduction robot.

Wang, Z., Yu, H., Shen, X., Xie, D., Wang, H. and Du, Z.
Superposition and Decomposition Analysis of Limbs' Vibration Based on 6-UPS Tibia Fracture Reduction Surgical Robot.
DOI: 10.5220/0012274600003807

In *Proceedings of the 2nd International Seminar on Artificial Intelligence, Networking and Information Technology (ANIT 2023)*, pages 86-92
ISBN: 978-989-758-677-4

2 KINEMATIC ANALYSIS OF THE STEWART PLATFORM

2.1 Inverse Kinematics of the Stewart Platform

Simplifying the 6-UPS fracture reduction surgical robot shown in **Fig. 1**, we obtain the robot coordinate system depicted in **Fig. 2**, where the hinge points on the moving and static platforms are positioned on two planes. The hinge points of the static platform are represented by $B_i(i = 1,2,\cdots,6)$, the hinge points of the moving platform are represented by$A_i(i = 1,2,\cdots,6)$.

Then the coordinates of the hinge point on the fixed platform in the fixed coordinate system can be expressed as:

$$B_i = [b_{xi} \quad b_{yi} \quad 0]^T = [R_b\cos\varphi_{bi} \ \ R_b\sin\varphi_{bi} \ \ 0]^T (i = 1,\ 2,\ \cdots,\ 6) \quad (1)$$

Then the coordinates of the hinge point on the moving platform in the moving coordinate system can be expressed as:

$$A_i = [a_{xi} \quad a_{yi} \quad 0]^T = [R_p\cos\varphi_{pi} \ \ R_p\sin\varphi_{pi} \ \ 0]^T (i = 1,\ 2,\ \cdots,\ 6) \quad (2)$$

The pose of the moving platform relative to the fixed platform is represented by a homogeneous transformation matrix T:

$$T = \begin{bmatrix} \cos\beta\cos\gamma & \sin\alpha\sin\beta\cos\gamma - \cos\alpha\sin\gamma & \cos\alpha\sin\beta\cos\gamma + \sin\alpha\sin\gamma & x_0 \\ \cos\beta\sin\gamma & \sin\alpha\sin\beta\sin\gamma + \cos\alpha\cos\gamma & \cos\alpha\sin\beta\sin\gamma - \sin\alpha\cos\gamma & y_0 \\ -\sin\beta & \sin\alpha\cos\beta & \cos\alpha\cos\beta & z_0 \\ 0 & 0 & 0 & 1 \end{bmatrix} \quad (3)$$

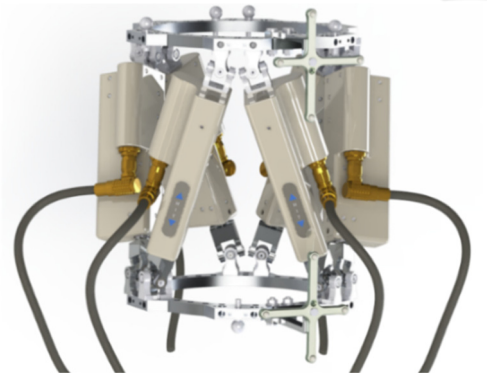

Figure 1: Robot Integration Diagram.

The expression of hinge point coordinates in the static coordinate system is as follows:

$$^{\psi_b}A_i = P + R \cdot {}^{\psi_p}A_i \quad (4)$$

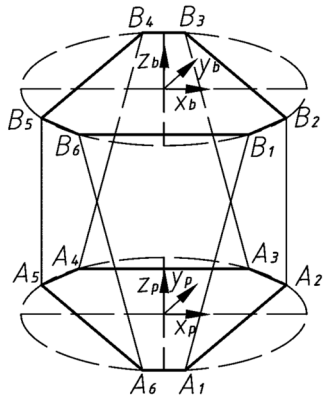

Figure 2: Coordinate System of Stewart Platforms.

The rod length of each drive rod of a parallel robot can be expressed as:

$$L_i\vec{n}_i = P_i + R \cdot {}^{\psi_p}A_i - {}^{\psi_b}B_i \quad (5)$$

In the equation:
$\vec{n_i}$—— the direction vector of the drive rodB_iA_i;
L_i——The length of the drive rodB_iA_i.

The inverse expression that can obtain the robot rod length is:

$$l_i = |A_iB_i| = \sqrt{\left\|P_i + R \cdot {}^{\psi_p}A_i - {}^{\psi_b}B_i\right\|^2} \quad (6)$$

The specific expression of the inverse rod length can be obtained:

$$l_i = \sqrt{(a_{xi}r_{11} + a_{yi}r_{12} + x_p - b_{xi})^2 + (a_{xi}r_{21} + a_{yi}r_{22} + y_p - b_{yi})^2 + (a_{xi}r_{31} + a_{yi}r_{32} + z_p)^2} \quad (7)$$

2.2 Positive Kinematics of the Stewart Platform

To improve the operation speed of kinematics when controlled by parallel robots, the solution of positive kinematics is iteratively solved by Newton's method (Liang, 2022).

For a given pose of a parallel robot $q = (x_p \quad y_p \quad z_p \quad \alpha \quad \beta \quad \gamma)^T$, the inverse kinematics equation can be converted to:

$$f_i(q) = (a_{xi}r_{11} + a_{yi}r_{12} + x_p - b_{xi})^2 + \cdots (a_{xi}r_{21} + a_{yi}r_{22} + y_p - b_{yi})^2 + (a_{xi}r_{31} + a_{yi}r_{32} + z_p)^2 - l_i^2 = 0 \quad (i = 1 \cdots 6) \quad (8)$$

Combine the equations of the six rods to get a system of equations:

$$F(q) = (f_1(q) \quad f_2(q) \quad f_3(q) \quad f_4(q) \quad f_5(q) \quad f_6(q))^T = 0 \quad (9)$$

Newton's method for solving a system of nonlinear equations can be expressed as:

$$q^{k+1} = q^k - [F'(q^k)]^{-1} F(q^k) \quad (10)$$

where $F'(q)$ is the equation derivation of each element, which can be expressed as:

$$F'(q) = \begin{bmatrix} \frac{\partial f_1(q)}{\partial x_p} & \frac{\partial f_1(q)}{\partial y_p} & \cdots & \frac{\partial f_1(q)}{\partial \gamma} \\ \frac{\partial f_2(q)}{\partial x_p} & \frac{\partial f_2(q)}{\partial y_p} & \cdots & \frac{\partial f_2(q)}{\partial \gamma} \\ \vdots & \vdots & \ddots & \vdots \\ \frac{\partial f_6(q)}{\partial x_p} & \frac{\partial f_6(q)}{\partial y_p} & \cdots & \frac{\partial f_6(q)}{\partial \gamma} \end{bmatrix} \quad (11)$$

After giving the member length of the six rods of the parallel robot, given the initial pose q_0 of the iteration, and specifying the iteration accuracy ε and the maximum number of iterations N, the posture that meets the requirements is obtained through iterative operation.

3 DYNAMICS ANALYSIS OF 6-UPS STEWART PLATFORM

The linear vibration unit can directly convert electrical energy into mechanical energy, driving the spring-mass block for linear motion, and avoiding radial vibrations. It provides delicate vibrations, fast startup speed, controllable direction, and obvious advantages. It is suitable for use as a vibration unit in fracture rehabilitation. Its internal structure is shown in **Fig. 3**. We can design a flange fixture as shown in **Fig. 4** to install the linear vibration motors in the limbs. As shown in **Fig. 5**, we have installed the motors fixture designed in the limbs.

The general idea of using the Newton-Euler method to establish the dynamic model of the 6-UPS platform is: assuming that the motion acceleration and angular acceleration of the required upper platform are known, the vector relationship in the fixed coordinate system is represented by the rotation matrix and the coordinate transformation matrix; Through the analysis of the kinematics and dynamics of the outrigger, the Newton-Euler dynamic equation of the outrigger is established, and the force of each leg on the upper platform is substituted into the Newton-Euler equation established on the upper platform, and the closed-loop dynamic equation of the entire platform is simplified and finally obtained. Performing dynamic analysis on a single rod as shown in **Fig. 6**.

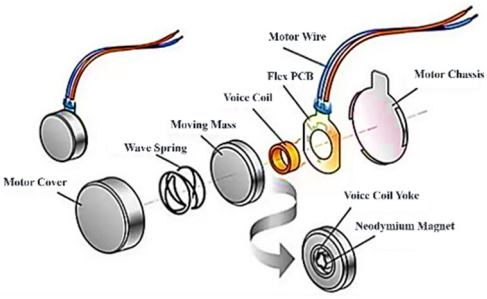

Figure 3: Internal Structure of Linear Motor.

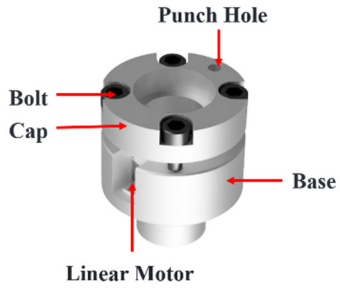

Figure 4: Linear Motor Connectors.

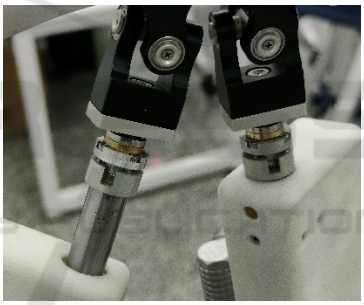

Figure 5: Linear Motor Physical Object.

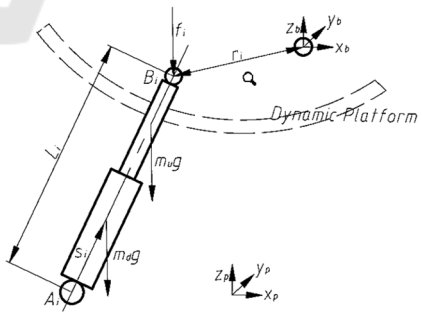

Figure 6: Single Branch Limb Force Analysis.

Taking the first $i$leg as the research object, the force analysis is shown in Figure 2, and the force balance equation is as follows:

$$m_u s_i \cdot a_{ui} = F_i + m_u s_i \cdot g - f_i, (i = 1, \cdots, 6) \quad (12)$$

In the equation:F_i is the driving force of the limb motor end; m_u is the mass of the limb pusher; $s_i$is the direction vector of the limb; g is the gravitational acceleration; a_{ui} is the acceleration of the pusher end of the limb; the force of the platform on the limb is f_i.

Taking the moving platform as the research object, the dynamic equilibrium equation is:

$$m_p a_p = m_p g + F_E + \sum_{i=1}^{6} f_i \quad (13)$$

In the equation:m_p is the mass of the moving platform; the center of mass acceleration of the moving platform is; the external force acting on the moving platform is F_E. Substituting equation (12) into equation (13), we obtain:

$$\sum_{i=1}^{6} F_i = m_p \alpha_p - m_p g - F_E + \sum_{i=1}^{6}(m_u s_i \cdot a_{ui} - m_u s_i \cdot g) \quad (14)$$

Similar to force balancing, the moment balance equation for the first limb is as follows:

$$(m_d r_{ui} + m_u r_{ai}) \times g - L_i s_i \times f_i - m_d r_{di} \cdot a_{di} - \omega_i \times (I_{di} + I_{ui}) - (I_{di} + I_{ui})\alpha_i - \omega_i m_u r_{ui} \times a_{ui} = 0 \quad (15)$$

In the equation: m_d is the mass at the motor end of the limb; $L_i$is the length of the limb motor end; r_{di} and r_{ui} are position vectors from point B_i to the fixed part and the movable part of the motor, respectively. I_{di} and I_{ui} are the inertia matrices of the fixed part and the movable part of the limb around the point B_i, respectively. ω_i and α_i are the angular velocity and angular acceleration of the limb, respectively.

Taking the moving platform as the research object, the moment balance equation of the moving platform is listed:

$$I_p a_p + \omega_p \times (I_P \omega_P) - M_E - r \times F_E = \sum_{i=1}^{6}[(\mathrm{Rb}_i) \times f_i] \quad (16)$$

In the equation: $m_p$is the quality of the moving platform; I_p is the inertia matrix of the moving platform; $M_E$is the external moment acting on the moving platform; ω_p, anda_p are angular velocity and angular acceleration of the moving platform; R is the transformation matrix for the coordinate system. Substituting equation (15) into equation (16), we obtain:

$$\sum_{i=1}^{6} \mathrm{Rb}^i \times (m_u s_i \cdot a_{ui} - m_u s_i \cdot g) + I_p a_p + \omega_p \times (I_p \omega_p) - M_E - r \times F_E = \sum_{i=1}^{6}[(Rb_i) \times F_i] \quad (17)$$

Combining the force balance equation (14) and the moment equilibrium equation (17) gives a dynamic equation of the following form:

$$H \cdot F = K \quad (18)$$

In the equation :

$$K = \begin{bmatrix} m_p a_p - m_p g - F_E + \sum_{i=1}^{6}(m_u s_i \cdot g - m_u s_i \cdot a_{ui}) \\ \sum_{i=1}^{6} Rb_i \times (m_u s_i \cdot a_{ui} - m_u s_i \cdot g) + I_p a_p + \omega_p \times (I_p \omega_p) - M_E - r \times F_E \end{bmatrix} \quad (19)$$

$$H = \begin{bmatrix} s_1 & s_2 & s_3 & s_4 & s_5 & s_6 \\ b \times s_1 & b_2 \times s_2 & b_b \times s_3 & b_4 \times s_4 & b_5 \times s_5 & b_b \times s_6 \end{bmatrix} \quad (20)$$

4 SUPERPOSITION AND DECOMPOSITION OF LIMB VIBRATIONS

4.1 Superposition of Vibrations

After the completion of the fracture reduction surgery, assuming the posture of the moving platform is known, we can obtain the direction vectors of the six branches. Based on the forward kinematics model, assuming that the vibration transmission time from the six branches to the moving platform is the same, we multiply the vibrations of the six branches by the decomposition of the unit direction vectors of each branch. This yields the vibrational components in the x, y, and z directions. By representing these components in three-dimensional space, we can observe the following laws as shown in **Fig. 7**.

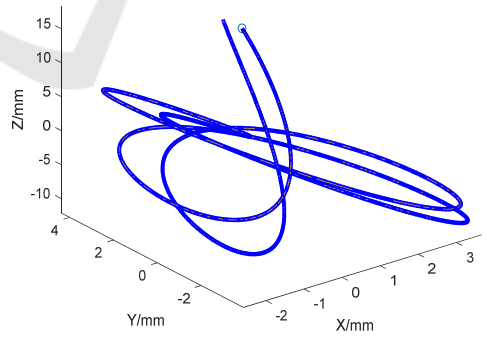

Figure 7a: Frequency is different, but amplitude and phase are the same.

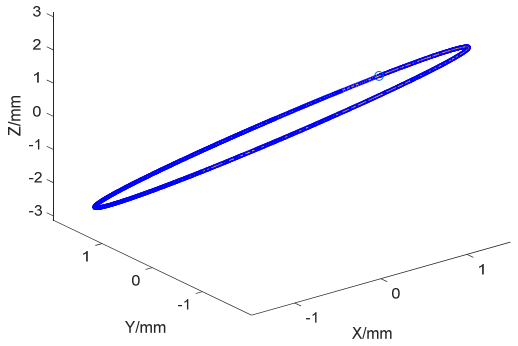

Figure 7b: Phase is different but amplitude and frequency are the same.

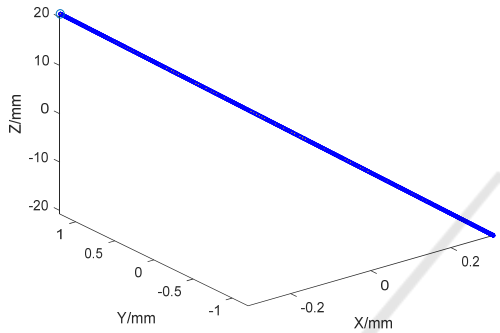

Figure 7c: Amplitude is different, but phase and frequency are the same.

It can be seen from the analysis that if you want the robot moving platform to vibrate in the direction of the force line, it is necessary to control the vibration phase and frequency of each limb consistently and adjust the direction of vibration by changing the amplitude. Calculating the amplitude of each limb needs to use the previously derived inverse kinematics formula.

4.2 Decomposition of Vibrations

Vibration decomposition assumes that the moving platform vibrates along the direction of the force line after fracture reduction. It decomposes the desired linear vibration of the moving platform. One approach is to move the moving platform a small distance along the force line direction and then study the coordinate changes of each branch, calculate the distance between the hinge points of the moving platform and the fixed platform, and observe the changes in the length of the branches. Another approach is to add the displacement of the moving platform to the initial pose of the robot, substitute the new pose into the previously calculated inverse kinematics model, and calculate the difference between the branches before and after to obtain the change in rod length. The results obtained by these two methods are consistent.

Pair pose X=2; Y=2; Z=2; ROLL=pi/15; PITCH=pi/12; YAW=pi/18. To facilitate the observation of the magnitude of the amplitude, we adjust the amplitude to 1μm, assume that the dynamic platform vibrates along the force line, and its vibration equation is 0.001sin(2t+2*pi/3). The rod length change of each rod calculated by the two methods is shown in **Fig. 8**, and the vibration of a single axis can be found to be close to sinusoidal, as shown in **Fig. 9**.

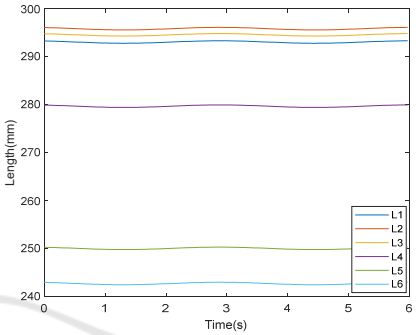

Figure 8: The length of the six limbs varies.

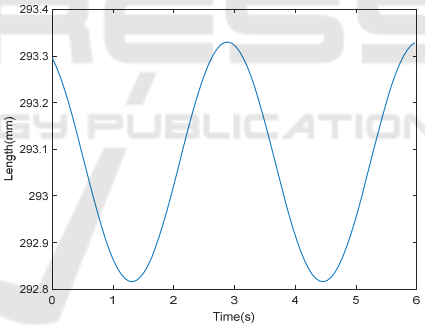

Figure 9: The length of a single limb varies.

5 DYNAMIC SIMULATION BASED ON ADAMS

Simplify the model and import it into ADAMS. Set the material properties and designate the push rod as the driver. Substitute the vibration equations of each supporting branch obtained in the previous chapter into the drivers of each rod. Conduct simulations and measure the force status of each rod component to obtain **Fig. 10**. Compare the results of dynamic numerical calculations with the results obtained from ADAMS simulations, as shown in **Fig. 11**. It can be observed that the numerical calculations and

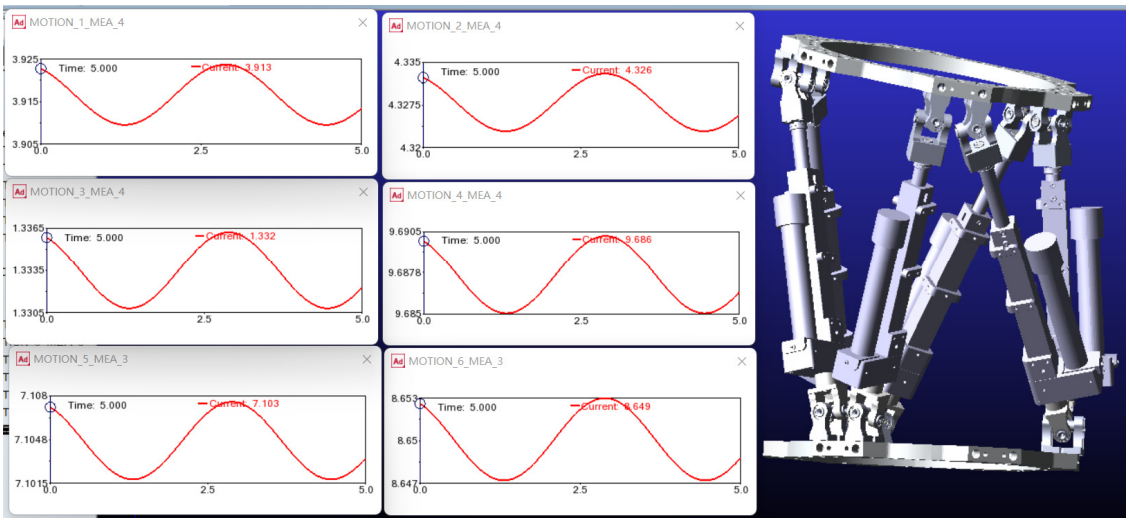

Figure 10: ADAMS simulation interface and results.

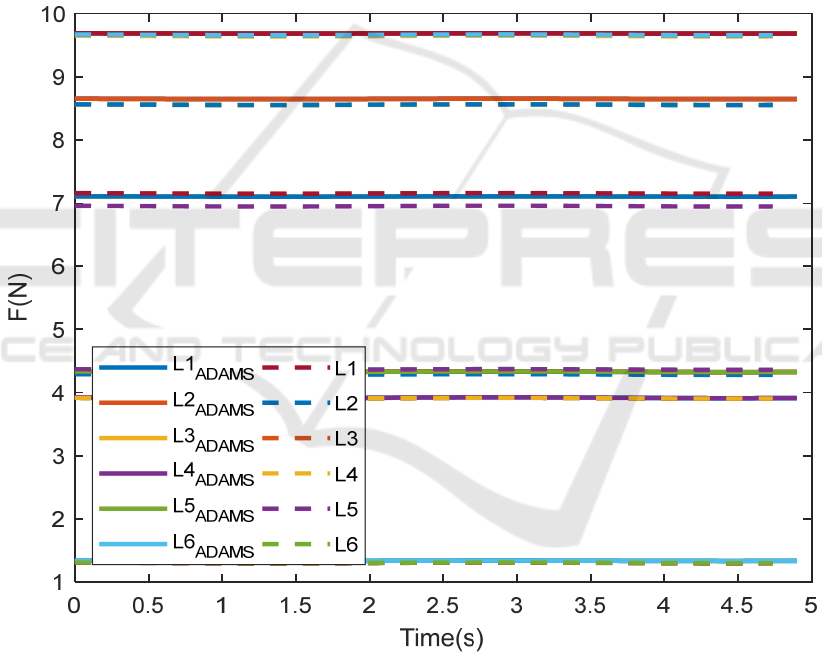

Figure 11: Comparison between ADAMS simulation and numerical calculation..

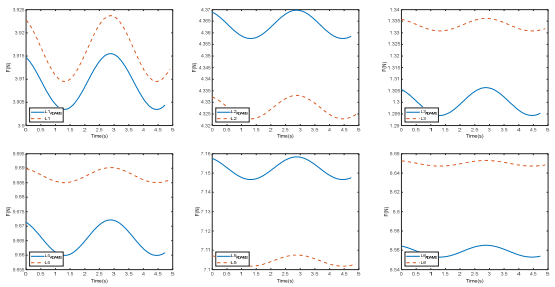

Figure 12: The vibration conditions of each component after magnification.

simulations yield similar results. Perform separate analysis and comparison of the dynamic calculation results for each bar, and obtain Fig. 12 . The calculation results indicate that within a margin of error not exceeding 0.7%, it can be reasonably assumed that the model is accurate.

6 CONCLUSION

This paper establishes the inverse kinematic model

and forward kinematic model of the 6-UPS Stewart platform to solve the vibration repair function required for tibial fracture reduction in the current 6-UPS robot. Based on the existing 6-UPS tibial fracture reduction robot, the installation of the linear vibration device on the limbs is analyzed. Under the condition of force-line direction vibration output by the motion platform, the synthesis of the limbs' vibration is achieved through forward kinematics, and the vibration conditions of each limb are verified under different vibration conditions. If the motion platform of the robot needs to undergo linear vibration along the force line, it is necessary to control the phase and frequency consistency of each limb vibration and adjust only the amplitude to change the vibration direction. Then, based on the inverse kinematics, the linear vibration set on the motion platform is decomposed, and the vibration equation of the linear vibration unit installed on each limb is obtained. Finally, based on the Newton-Euler method, the analysis of the 6-UPS tibial fracture reduction robot is completed, and the model is validated using ADAMS. The calculation results show that within an error range of not exceeding 0.7%, the model can be reasonably considered accurate. This paper provides a theoretical basis for improving the rehabilitation function of tibial fracture reduction robot through vibration.

ACKNOWLEDGMENTS

This work was financially supported by the Key-Area Research and Development Program of Guangdong Province (No.2020B0909020002) and Self-Planned Task (No.SKLRS202211B) of State Key Laboratory of Robotics and System (HIT).

REFERENCES

Ye R, Chen Y, Yau W. A simple and novel hybrid robotic system for robot-assisted femur fracture reduction[J]. *Advanced Robotics*, 2012, 26(1-2): 83-104. https://doi.org/10.1163/ 016918611x607383

Westphal R, Winkelbach S, Gösling T, et al. A surgical telemanipulator for femur shaft fracture reduction[J]. *The International Journal of Medical Robotics and Computer Assisted Surgery*, 2006, 2(3): 238-250.https://doi.org/10.1002/rcs.81

Westphal R, Winkelbach S, Wahl F, et al. Robot-assisted long bone fracture reduction[J]. *The International Journal of Robotics Research*, 2009, 28(10): 1259-1278. https://doi.org/10.1177/ 0278364909101189

Oszwald M, Westphal R, Bredow J, et al. Robot-assisted fracture reduction using three-dimensional intraoperative fracture visualization: An experimental study on human cadaver femora[J]. *Journal of Orthopaedic Research*, 2010, 28(9): 1240-1244.https://doi.org/10.1002/ jor.21118

Liodakis E, Chu K, Westphal R, et al. Assessment of the accuracy of infrared and electromagnetic navigation using an industrial robot: Which factors are influencing the accuracy of navigation? [J]. *Journal of Orthopaedic Research*, 2011, 29(10): 1476-1483.https://doi.org/10.1002/jor.21429

Koo T K K, Chao E Y S, Mak A F T. Development and validation of a new approach for computer-aided long bone fracture reduction using unilateral external fixator[J]. *Journal of Biomechanics*, 2006, 39(11): 2104-2112. https://doi.org/10.1016/j.jbiomech.2005.06.002

Li C, Wang T, Hu L, et al. A novel master–slave teleoperation robot system for diaphyseal fracture reduction: a preliminary study[J]. *Computer Assisted Surgery*, 2016, 21(sup1): 162-167. https://doi.org/10.1080/24699322.2016.1240304

Cai C, Zheng X, Shi M, et al. Bone collision detection method for robot assisted fracture reduction based on vibration excitation[J]. *Computer Methods and Programs in Biomedicine*, 2023, 229: 107317.https://doi.org/10.1016/j.cmpb.2022.107317

Liang F, Tan S, Zhao X, et al. Kinematics and Dynamics Simulation of a Stewart Platform[C]. *Journal of Physics: Conference Series*, 2022, 2333(1):012026. https://doi.org/10.1088/1742-6596/2333/1/012026